Mechanisms of causal interaction between short-term RR interval and systolic arterial pressure oscillations during orthostatic challenge

Luca Faes, Giandomenico Nollo and Alberto Porta

You might find this additional info useful...

This article cites 43 articles, 24 of which you can access for free at:
http://jap.physiology.org/content/114/12/1657.full#ref-list-1

Updated information and services including high resolution figures, can be found at:
http://jap.physiology.org/content/114/12/1657.full

Additional material and information about *Journal of Applied Physiology* can be found at:
http://www.the-aps.org/publications/jappl

This information is current as of June 16, 2013.

Mechanisms of causal interaction between short-term RR interval and systolic arterial pressure oscillations during orthostatic challenge

Luca Faes,[1] Giandomenico Nollo,[1] and Alberto Porta[2]

[1]*Department Physics and BIOTech Center, University of Trento, Trento, Italy; and* [2]*Department of Biomedical Sciences for Health, Galeazzi Orthopaedic Institute, University of Milan, Milan, Italy*

Faes L, Nollo G, Porta A. Mechanisms of causal interaction between short-term RR interval and systolic arterial pressure oscillations during orthostatic challenge. *J Appl Physiol* 114: 1657–1667, 2013. First published April 11, 2013; doi:10.1152/japplphysiol.01172.2012.—The transition from the supine to the upright position requires a reorganization of the mechanisms of cardiovascular control that, if not properly accomplished, may lead to neurally mediated syncope. We investigated how the patterns of causality between systolic arterial pressure (SAP) and cardiac RR interval were modified by prolonged head-up tilt using a novel nonlinear approach based on corrected conditional entropy (CCE) compared with the standard approach exploiting the cross-correlation function (CCF). Measures of coupling strength and delay of the causal interactions from SAP to RR and from RR to SAP were obtained in 10 patients with recurrent, neurally mediated syncope (RNMS) and 10 healthy control (CO) subjects in the resting supine position (*su*) and after head-up tilting during early (*et*; ~2 min) and late (*lt*; ~15 min or before presyncope) epochs of upright posture. Main results were that *1*) the coupling strength from SAP to RR increased significantly from *su* to *et* in both groups; by contrast, upon *lt*, the coupling strength was kept high in CO subjects and dropped to low values in RNMS patients; *2*) in RNMS patients, the delay from SAP to RR was higher than in healthy controls and increased moving from *et* to *lt*. Although these trends were evident using the CCE approach, statistical significance was not attained using the CCF approach. These results indicate the necessity of dissecting causality between RR and SAP to properly assess directional mechanisms from the closed-loop cardiovascular regulation and suggest a weakened and slowed baroreflex as a major mechanism involved in the cardiovascular impairment associated to neurally mediated syncope.

autonomic nervous system; baroreflex; conditional entropy; cross-correlation; head-up tilt; neurally mediated syncope; cardiovascular control

THE HEART PERIOD, COMMONLY assessed as the duration of the RR interval measured from the ECG, and the systolic arterial pressure (SAP) are known to reciprocally affect each other. This closed-loop interaction is the result of the baroreceptor-heart rate reflex (hereinafter, cardiac baroreflex) acting as a delayed negative feedback of SAP on RR interval to keep the arterial pressure around a preset value (6, 20) and of the feed-forward effect of RR interval on SAP variability occurring as a result of modifications of the ventricular filling and diastolic runoff (23, 36). These mechanisms are usually investigated noninvasively through the analysis of the coupling between RR and SAP spontaneous variability during experimental conditions challenging the baroreflex. One of these conditions is the orthostatic stress leading to a decrease of venous return and, consequently, to a tachycardic response

preventing the drop in arterial pressure. Under some circumstances, this postural challenge might lead to syncope (i.e., the loss of consciousness while standing) (4). Time series analysis methods applied to RR and SAP variability have been utilized to study modifications of the RR-SAP interactions during the development of postural syncope with the final aim of preventing its occurrence using countermeasures (13, 24, 26).

A major approach for the assessment of RR-SAP interactions is causality analysis. This analysis allows to evaluate the directional interactions due to the cardiac baroreflex feedback (i.e., from SAP to RR) separately from those due to the mechanical feed-forward (i.e., from RR to SAP), as well as to identify the dominant causal relation in the observed closed loop. The most used method for the assessment of causality between RR and SAP is based on the cross-correlation function (CCF), which provides measures of coupling strength and time delay of feedback and feed-forward effects when assessed over negative and positive time shifts (41, 47). However, the cross-correlation method provides an open-loop estimate of the strength of the RR-SAP relation. Open-loop approaches implicitly assume the existence of an input-output relationship between two variables, such that any observed interaction is ascribed to the input-output direction while the reverse direction is neglected (1). As a consequence, open-loop estimates of causality along a given direction may become unreliable when causal effects along the opposite direction are not negligible. In the case of cross-correlation, couplings and delays detected for positive and negative time shifts are not independent because the CCF oscillates at common frequencies of both RR and SAP series. Thus it is a common practice to select the most plausible delay according to prior information (e.g., the latency of the cardiac baroreflex). For example, if the delay of the relation from SAP to RR is not compatible with the baroreflex latency, the reverse causal relation is preferred and the delay from RR to SAP is retained as meaningful. Another limitation is that the CCF identifies exclusively the linear contributions to the relationships between RR and SAP, whereas nonlinear components are likely to be substantial in several circumstances. These limitations may endanger the interpretation of coupling strength and delay indexes measured from cross-correlation analysis of RR and SAP. In fact, recent studies have pointed out the need of adopting approaches that effectively test for causality and that may account for both linear and nonlinear couplings to study directional interactions between cardiovascular time series (10, 36, 46).

In this study, we apply measures taken from information theory to assess causality between RR and SAP during prolonged orthostatic stress. The approach is based on the assessment of the information transfer (39) from SAP to RR and vice versa. Its main peculiarities are the ability to deal with closed-

Address for reprint requests and other correspondence: L. Faes, Lab. Biosegnali, Dipartimento di Fisica & BioTech, Università di Trento, via delle Regole 101, 38060 Mattarello, Trento, Italy (e-mail: luca.faes@unitn.it).

loop interactions without assuming a priori the existence of any causal relationship and the ability to capture both linear and nonlinear interactions without specifying a model of the observed interactions. The specific tool used here, which is based on estimation of the corrected conditional entropy (CCE) (31), has been set and validated on several simulation schemes in Ref. 11 and tested on cardiovascular time series in Ref. 12. In the present study, it is exploited to quantify the strength of the causal coupling over the two directions of the closed loop between RR and SAP during three peculiar epochs of a tilt-test protocol in a group of patients with recurrent neurally mediated syncope (RNMS) and in a control group (CO) of healthy subjects. The approach also allows the quantification of the delay of the interaction from SAP to RR and from RR to SAP. The derived coupling and delay measures are compared with those obtained from the traditional CCF to assess the ability of the two approaches to reflect changes of the short-term cardiovascular regulation evoked by head-up tilt, as well as the impairment of this regulation related to the occurrence of neurally mediated syncope. Moreover, to complement the results of the proposed information-domain approach when applied over the feedback direction from RR to SAP, the coupling and sensitivity of the cardiac baroreflex were investigated by a more traditional time-domain approach based on the sequence technique (8, 28).

METHODS

Subjects and experimental protocol. All subjects and patients enrolled in the study provided informed consent to the experimental protocol, which conformed to the principles of the Declaration of Helsinki and was approved by the Ethical Committee of the hospital. The study population consisted of 10 patients (4 men and 6 women, age range = 15–71 yr, mean 37 ± 17 yr) admitted to the syncope unit of the S. Chiara hospital of Trento, Italy, for the evaluation of RNMS (i.e., more than three syncope events during the foregoing year). The diagnosis of RNMS was established after a review of the patient's medical history, a comprehensive physical examination, and a positive response to head-up tilt table testing. Patients had previously been investigated with 12-lead ECG and Holter monitoring, and some also had cardiac echocardiograms and/or electroencephalogram when considered clinically appropriate. Results of all tests did not indicate any cardiovascular or neurological disease. Patients were not taking any medication affecting cardiovascular control at the time of the study. The CO group consisted of 10 age- and sex-matched healthy subjects (4 men and 6 women, 31 ± 10 yr, P = not significant vs. patients) with no previous history of syncope and no clinical evidence of any other cardiovascular disease, who were selected during the recruitment of CO subjects for tilt studies. All subjects did not take any medication and refrained from intake of caffeine or alcoholic beverages as well as from physical exercise in the 24 h before the study. All CO had negative response to head-up tilt test.

Head-up tilt test was performed in the late morning in a quiet room with controlled temperature (22–24°C) and ventilation, with subjects enrolled after ~5 h of fasting. Subjects, who were in sinus rhythm and breathing spontaneously, lay on a tilt table supported by two belts at the level of thigh and waist, and with both feet in contact with the footrest of the table. The protocol consisted of 5 min of rest in the supine position, 10 min of signal recording in the same position, passive transition to the upright position achieved by progressive sloping of the motorized tilt table in to the upright position (60° head up), and subsequent data acquisition in the upright position for a maximum of 30 min. If symptoms associated with presyncope occurred, the table was rapidly lowered to the horizontal position, and the test was labeled as positive. Presyncope was defined as a rapid

decrease in systolic pressure to below 90 mmHg associated with symptoms of dizziness, nausea, or diaphoresis. The signals acquired during the test were the ECG (lead II) and the continuous photoplethysmographic arterial pressure (Finapres, Ohmeda), which were digitized at 1-kHz sampling rate and 12-bit resolution. The arterial pressure signal was cross-calibrated in each session with the measure provided by a sphygmomanometer during the rest period in the supine position.

Cardiovascular variability series measurement and pre-processing. After detection of the QRS complexes from the ECG followed by location of the R apex through template matching, the RR interval was measured as the temporal distance between two consecutive R peaks. The corresponding systolic arterial pressure (SAP) was measured as the maximum of the arterial pressure signal inside the detected RR interval. The beat-to-beat variability series of RR and SAP, i.e., RR(n) and SAP(n), $n = 1, \ldots N$, were then measured as the sequences of consecutive RR intervals and SAP values measured during peculiar epochs of the tilt-test protocol. Specifically, three time windows, each lasting 300 beats, were selected for the analysis: one in the supine position (*su*) and two in the upright position, denoted respectively as early tilt (*et*) and late tilt (*lt*). To allow for subject stabilization after tilting, the *et* window was selected starting from ~2 min after the supine-to-upright transition. In RNMS patients, the *lt* window was chosen immediately before the decrease in SAP that was considered the hallmark of presyncope. In the CO group, the *lt* window was chosen starting at ~15 min, a period chosen on the basis of the mean duration of tilt (15 ± 8 min) in the group of RNMS patients. For each analyzed window, the occurrences of QRS and SAP were carefully inspected to avoid erroneous detections or missed beats. Moreover each time series was detrended using a zero-phase high-pass filter (with cutoff at 0.01 Hz). Representative examples of the RR and SAP series measured for the three windows in a CO subject and in a RNMS patient are reported in Fig. 1.

Traditional time- and frequency-domain analyses. To provide time-domain measures of variability for each single series, the mean and standard deviation of RR and SAP, denoted as μ_{RR}, μ_{SAP}, σ_{RR}, and σ_{SAP}, were calculated inside each observed window. Moreover, the square root of the mean squared differences of successive RR intervals (RMSSD) was computed to characterize short-term components of heart rate variability (42).

To assess heart rate variability in the frequency domain, spectral analysis of each measured RR interval series (42) was performed by means of the weighted covariance estimator, i.e., computing the Fourier transform of the autocorrelation function of the RR series multiplied by a smoothing window (here, we used the Hamming window with 0.03-Hz spectral bandwidth). The estimated spectral density function was then integrated over the low-frequency (LF; 0.04–0.15 Hz) and high-frequency (HF; 0.15–0.4 Hz) bands, and the HF power and LF-to-HF power ratio were measured as indexes of parasympathetic activity and sympathovagal balance, respectively.

The baroreflex modulation of heart rate was assessed in the time domain by means of the sequence technique (8, 28). Briefly, each measured SAP series was scanned, and we looked for sequences of three or more consecutive samples (denoted as ramps), during which SAP progressively increased or decreased at least 1 mmHg/beat. Then, for each detected SAP ramp, a corresponding SAP/RR sequence (i.e., a baroreflex sequence) was identified if the SAP ramp was followed after a lag of 0, 1, or 2 beats by a RR interval ramp in which RR exhibited progressive variations of at least 5 ms/beat with the same sign of the SAP variations for ≥3 consecutive beats. With these definitions, the baroreflex effectiveness index (BEI) is measured as the ratio between the number of baroreflex sequences (N_{seq}) and the number of SAP ramps (8), providing information on how often the cardiac baroreflex takes control of the sinus node in response to spontaneous SAP changes. Moreover, to investigate the sensitivity of the spontaneous baroreflex, we performed linear regression analysis between SAP and RR values from each identified SAP/RR sequence
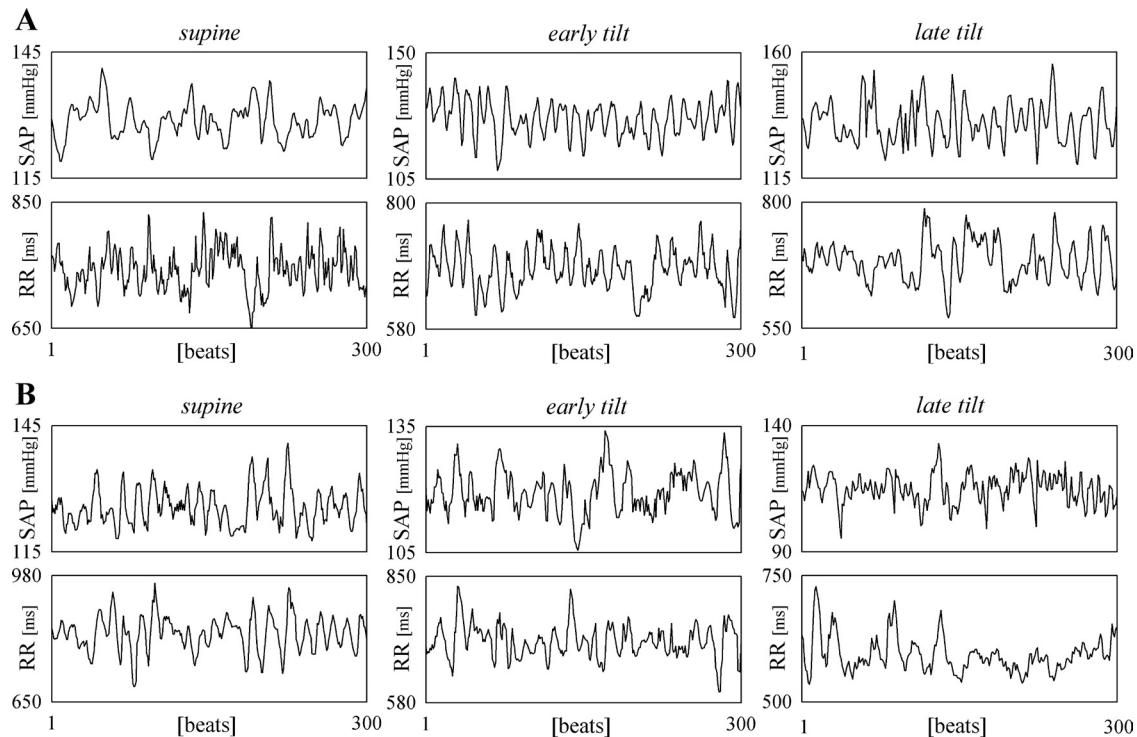
Fig. 1. Example of systolic arterial pressure (SAP) and RR interval series measured for a control (CO) subject (*A*) and for a recurrent neurally mediated syncope (RNMS) patient (*B*) in the three windows of the head-up tilt test protocol.

and then provided estimates of the baroreflex sensitivity averaging the slopes of the regression lines over all sequences (BRS index) or solely over the three-beats sequences (BRS$_3$ index).

Cross-correlation analysis. Cross-correlation analysis was performed according to the approach performed in Ref. 41. This approach is based on computing the cross-correlation function (CCF) between SAP and RR at varying the time shift between the two variables with the convention that negative time shifts identify the causal relation from SAP to RR (i.e., RR lags behind SAP) and positive time shifts identify the causal relation from RR to SAP (i.e., RR leads SAP). The raw CCF estimates were normalized by the product of the standard deviations of RR and SAP. The values of time lag (negative) and amplitude (positive) of the dominant CCF peak were calculated for time shifts between -25 and 0 beats, yielding the measures of delay and strength of the relation from SAP to RR, labeled as $\tau_{SAP \to RR}$ and $\rho_{SAP \to RR}$ in the following, and the values of time lag (positive) and amplitude (negative) of the dominant CCF valley were calculated for time shifts between 0 and 25 beats, yielding the measures of delay and strength of the relation from RR to SAP, labeled as $\tau_{RR \to SAP}$ and $\rho_{RR \to SAP}$ in the following. The absolute values of the negative amplitudes and time shifts were considered. Moreover, a measure of directionality was taken as the difference of the two causal couplings: $\Delta = \rho_{SAP \to RR} - \rho_{RR \to SAP}$. Figure 2 reports a representative example of cross-correlation analysis.

Information-domain analysis. Information-domain analysis was performed according to the approach proposed in Refs. 11 and 12. This approach is based on the concepts of entropy and conditional entropy. According to information-theoretic definitions (27), the entropy of the RR series (H_{RR}) quantifies the average uncertainty associated with its most recent sample, RR(n), whereas the entropy of the RR series conditioned to its own past, $H_{RR|RR}$, quantifies the average uncertainty that remains about the present sample RR(n) when its past samples, RR(n-k) with $k \geq 1$, are known; similarly, $H_{RR|RR,SAP}$ denotes the conditional entropy of the RR series given both its own past and that of the SAP series, i.e., SAP(n-k) with

$k \geq 0$. By reversing the role between RR and SAP, the entropy of SAP (H_{SAP}) and the conditional entropy of SAP given its past ($H_{SAP|SAP}$) or given both its past and the past of RR ($H_{SAP|SAP,RR}$) may be computed. Note that in the computation of $H_{RR|RR,SAP}$ the present sample of SAP, SAP(n), is considered together with the time-shifted samples to account for fast vagal modulations whereby SAP(n) affects RR(n) within the same beat through the cardiac baroreflex. On the contrary, the present sample of RR is not considered in the computation of $H_{RR|RR,SAP}$, because RR(n) cannot affect SAP(n) according to the adopted measurement convention [SAP(n) occurs before the end of RR(n)].

In this study, the conditional entropy was computed according to a sequential procedure for non-uniform conditioning, which is briefly illustrated in the following (we refer to Ref. 11 for a detailed description). The procedure starts with a set of initial candidate terms containing the past samples of the time series up to a maximum lag L_{max} ($L_{max} = 10$ in this study) and then picks up the terms to be used for computing the conditional entropy in a progressive way, selecting at each step the term that leads to the highest reduction in uncertainty of the time series under analysis, i.e., that leads to the minimum conditional entropy; the procedure terminates when the addition of a new term does not reduce the uncertainty of the target series, i.e., when a minimum in the conditional entropy is reached. As an example, let us consider the computation of $H_{RR|RR,SAP}$ in the example of Fig. 3*A* (gray lines): the procedure for describing RR from its past and the past of SAP starts from the set of candidates [RR(n-1), . . . , RR(n-10), SAP(n), SAP(n-1), . . . , SAP(n-10)], then selects progressively the terms RR(n-1), SAP(n), and RR(n-10) and terminates at the third step because the addition of a new term does not bring further reduction in uncertainty as measured by the conditional entropy. Therefore, in this example, the RR variability is best explained in terms of resolution of uncertainty by using the samples [RR(n-1), SAP(n), RR(n-10)] to describe RR(n).

As to the practical estimation of conditional entropy, we used the strategy set in Ref. 31. This strategy is based on performing a uniform quantization of the RR and SAP series over ξ quantization levels ($\xi =$

with the computation performed solely on the basis of the past of the target series (black lines). On the contrary, when no terms from the input series are selected, even when they are tested by the procedure, the two CCE profiles overlap so that the causal coupling is zero (e.g., see Fig. 3, *bottom left*) and the time delay is not computed.

Statistical analysis. The significance of each estimated causal coupling was assessed by means of a statistical test based on the generation of surrogate data. Specifically, the original value of the considered coupling measure (either $\rho_{SAP \to RR}$, $\rho_{RR \to SAP}$, $C_{SAP \to RR}$, $C_{RR \to SAP}$) was compared with the distribution of the same measure computed under the hypothesis of uncoupling, obtained by generating several pairs (50 in this study) of fully uncorrelated surrogate time series sharing the individual properties (i.e., amplitude distribution and Fourier spectrum) of the original series. The isospectral and isodistributed surrogate time series pairs were generated according to the iterative algorithm proposed in Ref. 40, and the test for significance was based on rank ordering assuming a 5% significance.

The statistical significance of variations of all computed indexes (see Table 1 and Figs. 4–6) across the three measurement windows (*su*, *et*, *lt*) was assessed by means of the Kruskal-Wallis nonparametric one-way ANOVA, followed by the Wilcoxon signed rank test for paired data as post hoc comparison between pairs of distributions;
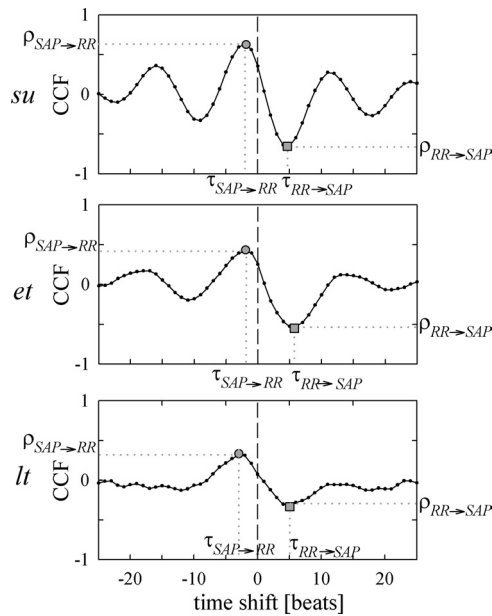
Fig. 2. Cross-correlation analysis between SAP and RR interval shown in the representative example of Fig. 1. In each panel, the dominant peak of the CCF is located for negative time shifts (circles), whereas the dominant valley is located for positive time shifts (squares). The magnitude and lag are taken as values of causal coupling and time delay from SAP to RR ($\rho_{SAP \to RR}$ and $\tau_{SAP \to RR}$, respectively) and from RR to SAP ($\rho_{RR \to SAP}$, $\tau_{RR \to SAP}$). The absolute values of $\tau_{SAP \to RR}$ and $\rho_{RR \to SAP}$ were considered for statistical analysis. The values obtained in this example are $\rho_{SAP \to RR} = 0.64$, $\tau_{SAP \to RR} = 2$, $\rho_{RR \to SAP} = 0.65$, $\tau_{RR \to SAP} = 5$ for the supine (*su*) window; $\rho_{SAP \to RR} = 0.42$, $\tau_{SAP \to RR} = 2$, $\rho_{RR \to SAP} = 0.53$, $\tau_{RR \to SAP} = 6$ for the early (*et*) window; and $\rho_{SAP \to RR} = 0.32$, $\tau_{SAP \to RR} = 3$, $\rho_{RR \to SAP} = 0.30$, $\tau_{RR \to SAP} = 5$ for the late (*lt*) window.

6 in this study) to get a first conditional entropy estimate, and then on adding to this estimate a correction that compensates for the bias that is known to affect conditional entropy progressively at increasing the number of conditioning terms. Besides counteracting this unreliability of conditional entropy, which is particularly problematic for short cardiovascular variability series, the resulting corrected conditional entropy (CCE) estimator serves in this study also to guarantee the existence of a minimum that allows terminating our procedure for sequential conditioning before the inclusion of irrelevant terms.

The procedure described above was used to compute information-theoretic measures of strength and delay of the causal interactions between each pair of RR and SAP series. In particular, the causal coupling from SAP to RR was defined as $C_{SAP \to RR} = (H_{RR|RR} - H_{RR|RR,SAP})/(H_{RR|RR})$, quantifying the reduction in uncertainty about $RR(n)$ that is brought exclusively by the knowledge of the past of SAP, normalized between 0 (the past of SAP does not resolve anything about the uncertainty of RR, which is not already resolved by its own past) and 1 (the whole uncertainty remaining in RR given its own past is resolved by the past of SAP). In a similar way, the causal coupling from RR to SAP was defined as $C_{RR \to SAP} = (H_{SAP|SAP} - H_{SAP|SAP,RR})/(H_{SAP|SAP})$, and a directionality measure was taken as the difference between the two causal couplings: $D = C_{SAP \to RR} - C_{RR \to SAP}$. The time delay from SAP to RR ($t_{SAP \to RR}$) was taken as the lag of the first candidate (if any) selected by the conditioning procedure among the past samples of SAP in the computation of $H_{RR|RR,SAP}$. Similarly, the time delay from RR to SAP ($t_{RR \to SAP}$) was taken as the lag of the first candidate (if any) selected among the past samples of RR in the computation of $H_{SAP|SAP,RR}$. An example of the whole information-domain analysis is reported in Fig. 3. Note that, in the computation of the CCE of the target series given the past of both series (gray lines), the selection of one or more terms from the past of the input series leads to a reduction of the CCE minimum compared
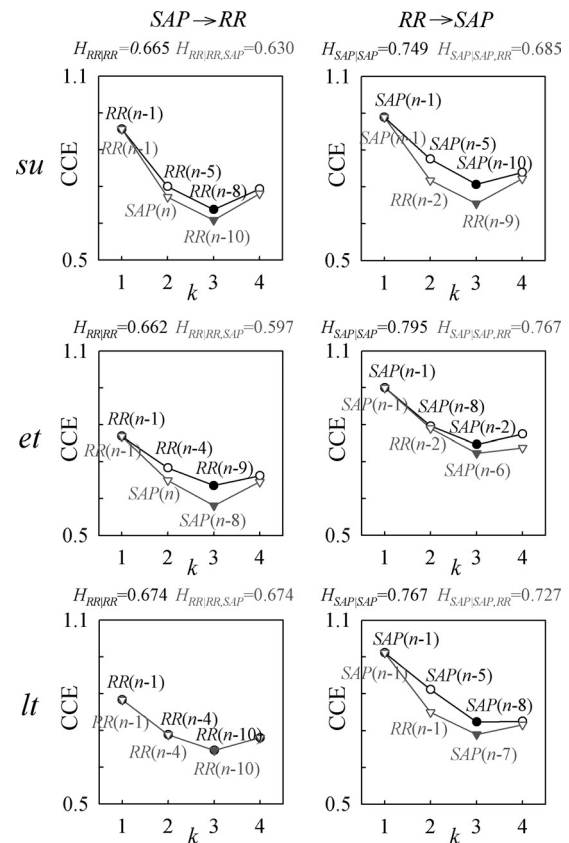

Fig. 3. Information domain analysis performed for the series of the CO subject shown in Fig. 1. Each panel reports the CCE of the RR series (*left*) and SAP series (*right*), conditioned to its own past (filled circles) and to both its own past and the past of the other series (gray triangles), computed at each step k of the non-uniform conditioning procedure (see text for details). The minimum CCEs are indicated with filled symbols, and the corresponding values are reported above the panel. The candidate components selected at each step k are also indicated in the panel. The values of causal coupling (C) and time delay (t) obtained in this example are $C_{SAP \to RR} = 0.053$, $t_{SAP \to RR} = 0$, $C_{RR \to SAP} = 0.085$, $t_{RR \to SAP} = 2$ for the *su* window (*top*); $C_{SAP \to RR} = 0.098$, $t_{SAP \to RR} = 0$, $C_{RR \to SAP} = 0.035$, $t_{RR \to SAP} = 2$ for the *et* window (*middle*); and $C_{SAP \to RR} = 0$, $t_{SAP \to RR} = $ na, $C_{RR \to SAP} = 0.052$, $t_{RR \to SAP} = 1$ for the *lt* window (*bottom*).

Table 1. *Summary of traditional time- and frequency-domain analyses*

	CO Subjects			RNMS Patients		
	su	*et*	*lt*	*su*	*et*	*lt*
μ_{RR}, ms	846 (749–899)	670* (648–758)	659* (644–689)	836 (719–1067)	720* (610–790)	619*† (551–743)
σ_{RR}, ms	34.9 (27.6–47.1)	43.6 (36.4–56.7)	38.6 (26.5–55.9)	38.8 (22.7–49.9)	26.6 (17.4–34.0)	16.4* (14.0–25.7)
RR RMSSD, ms	27.6 (19.0–34.9)	18.4 (10.6–27.2)	18.3 (10.9–25.5)	24.3 (11.0–41.1)	13.1* (6.3–17.8)	7.5*† (5.1–10.5)
RR HF power, ms^2	344.3 (156–638)	199.9 (123–375)	168.3 (78–296)	295.4 (41–567)	72.6* (39–137)	32.7*† (20–64)
RR LF/HF ratio, a.u.	1.7 (1.0–1.9)	6.5* (4.6–8.4)	6.8* (5.3–9.5)	2.1 (1.8–2.4)	5.5* (4.5–6.8)	5.0 (5.0–7.9)
μ_{SAP}, mmHg	113.8 (108–131)	118.1 (106–127)	116.5 (109–135)	129.3 (126–133)	117.6* (109–123)	110.4*† (99–125)
σ_{SAP}, mmHg	4.3 (3.6–5.3)	5.5* 4.2–6.9	6.8* (5.9–7.8)	3.8 (3.2–4.1)	5.1 (3.4–5.7)	5.3 (3.7–6.5)
BRS, ms/mmHg	13.70 (8.77–17.11)	6.62* (5.80–8.10)	6.07* (5.43–6.33)	10.14 (4.52–16.66)	5.84* (3.87–7.22)	3.36*† (2.81–4.96)
BRS$_3$, ms/mmHg	14.06 (8..55–17.52)	6.52* (5.51–8.01)	5.67* (5.09–6.26)	10.50 (4.56–16.99)	5.57* (4.02–7.23)	3.42*† (2.80–5.05)
BEI, n.u.	0.51 (0.36–0.58)	0.64 0.49–0.67	0.49 (0.38–0.57)	0.34 (0.24–0.47)	0.46 (0.39–0.57)	0.16*† (0.09–0.25)

Values are median (first quartile to third quartile) of the RR interval mean (μ_{RR}), standard deviation (σ_{RR}), square root of the mean squared differences (RMSSD), high-frequency (HF) power, and low-frequency-to-high-frequency power ratio (LF/HF), the systolic arterial pressure mean (μ_{SAP}) and standard deviation (σ_{SAP}), the overall baroreflex sensitivity (BRS) and the baroreflex sensitivity of the three-beats sequences (BRS$_3$), and the baroreflex effectiveness index (BEI) from sequence analysis, measured in the supine position (*su*) and in the upright position during early tilt (*et*) and late tilt (*lt*) windows for control (CO) subjects and recurrent neurally-mediated syncope (RNMS) patients. *Statistically significant difference of *su* vs. *et* and *su* vs. *lt* ($P < 0.05$). †Statistically significant difference *et* vs. *lt* ($P < 0.05$).

correction for multiple comparisons in the post hoc tests was performed according to the sequential Bonferroni approach introduced by Holm (18). The Wilcoxon signed rank test for paired data was used to assess the significance of each directionality index (Δ or D), i.e., to test the hypothesis that the values measured for the index come from a distribution with zero median.

The statistical analysis was performed for the time delay indexes ($\tau_{SAP \rightarrow RR}$, $\tau_{RR \rightarrow SAP}$, $t_{SAP \rightarrow RR}$, $t_{RR \rightarrow SAP}$) also after pooling together the data coming from the three windows (*su*, *et*, *lt*). The analysis of pooled data was performed by applying the Wilcoxon rank sum test for equal medians (Mann-Whitney *U*-test) to test the statistical significance of the difference between CO subjects and RNMS patients for a given delay index, and of the difference between the delay indexes over the two opposite causal directions ($\tau_{SAP \rightarrow RR}$ vs. $\tau_{RR \rightarrow SAP}$ or $t_{SAP \rightarrow RR}$ vs. $t_{RR \rightarrow SAP}$) for a given group.

RESULTS

Table 1 reports the median (25th to 75th percentile) of the distribution of the time-domain measures of RR and SAP variability in the two groups. The CO subjects showed the typical response to head-up tilt, documented by the maintenance of the mean SAP values accompanied by tachycardia (significant decrease in the mean RR) moving from the *su* to the upright position; the mean values did not change significantly in the *lt* window compared with the *et* window. On the contrary, in RNMS patients, a progressive decrease both in the mean RR and in the mean SAP was observed moving from *su* to *et* and then to *lt* windows, suggesting an inability of the cardiovascular control to maintain arterial pressure with prolongation of the orthostatic stimulus. Hypotension continued progressively after the *lt* window, with SAP first dropping below 90 mmHg and then being recovered upon tilting the table back to the supine position. The variability of RR did not change significantly across the three windows in the CO subjects, whereas a decrease during *lt* was observed for the RNMS patients. The two groups also showed an increase of SAP variability moving from the supine to the upright position, which was statistically significant only for the CO subjects.

The RR interval LF-to-HF power ratio increased significantly with tilt in both groups, indicating a shift toward sympathetic activation and parasympathetic deactivation in the upright position. Moreover, the RR HF power was reduced in

the upright position in CO subjects, although the variation was not significant and decreased progressively and significantly from *su* to *et* to *lt* in RNMS patients. The same trends were found in the time domain looking at the RMSSD of the RR intervals, documenting a loss of parasympathetic activity in the upright position and upon presyncope. These trends were also confirmed by the estimates of baroreflex sensitivity, since both BRS and BRS$_3$ decreased significantly from *su* to *et* in the two groups and decreased even further during *lt* in the RNMS patients. An additional indication of the baroreflex dysfunction before presyncope was provided by the marked decrease of the BEI index observed in the RNMS group during the *lt* window, reflecting the impaired effectiveness of the cardiac baroreflex in driving the sinus node in this condition.

Figure 4 depicts the results of causal coupling analysis performed using the cross-correlation approach and the information-domain approach. In the CO group, the two approaches show similar trends of the causal coupling from SAP to RR (measured by $\rho_{SAP \rightarrow RR}$ and $C_{SAP \rightarrow RR}$): the coupling strength increased significantly, moving from the *su* to the *et* window, and was kept at high values during *lt*. By contrast, in RNMS patients, the information theoretic approach showed a significant increase of the causal coupling from *su* to *et* followed by a significant decrease in the *lt* window. These trends were not clear using the cross-correlation approach. A different behavior between the two approaches was observed for the coupling strength over the opposite direction from RR to SAP: whereas the index $\rho_{RR \rightarrow SAP}$ measured by cross-correlation analysis did not show any statistically significant variation across the three windows in both groups, in CO subjects the index $C_{RR \rightarrow SAP}$ measured by information-domain analysis was significantly higher during *su* than during *et* and *lt*. All these results were reinforced by the significance analysis performed using surrogate data, evidencing variations across the three windows of the number of subjects or patients showing significant causal coupling that were in agreement with the variations of the measured coupling strengths (Table 2). The directionality index evaluated in the CO group through cross-correlation analysis (Fig. 4*A*, *bottom*) did not evidence a preferential coupling direction in the *su* window (Δ was not significant) and increased moving to the *et* and *lt* windows so that the preferential

Fig. 4. Results of causal coupling analysis performed by the cross-correlation approach (*A*) and by the information-domain approach (*B*). Plots report the individual values of the causal coupling from SAP to RR (top, circles) and from RR to SAP (middle, squares), and of the directionality index (bottom, triangles) computed for CO subjects and RNMS patients in the *su*, *et*, and *lt* windows of the tilt-test protocol. Filled symbols indicate values of causal coupling detected as statistically significant according to surrogate data analysis. #Statistically significant difference of *su* vs. *et*, *su* vs. *lt*, or *et* vs. *lt* ($P < 0.05$). *Statistically significant directionality index.
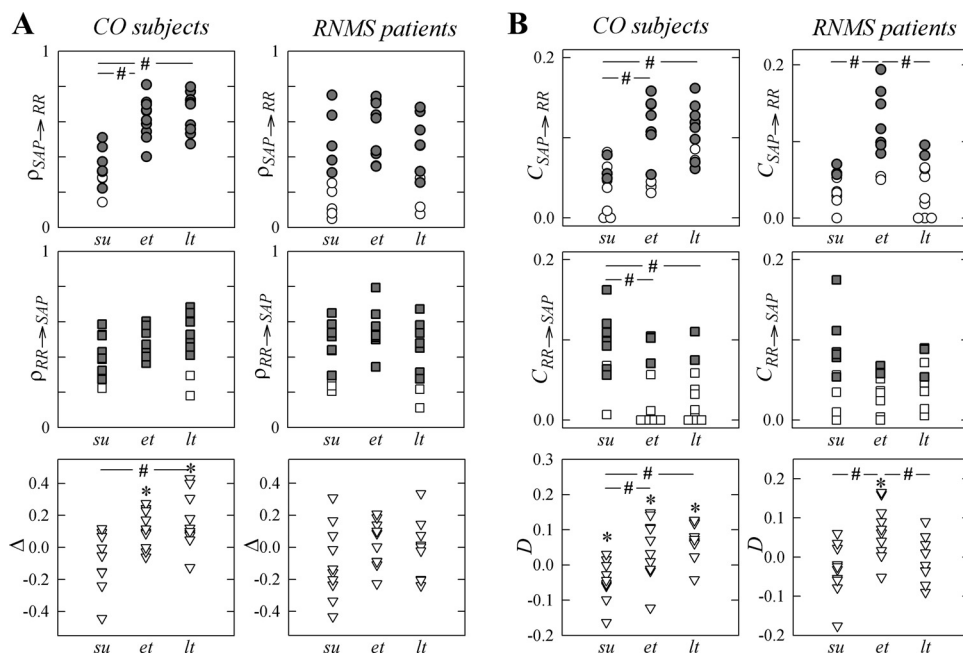
coupling direction was set from SAP to RR during tilt. The same index computed for RNMS patients was not significant and did not change across the three windows. When computed through information-domain analysis (Fig. 4*B*, *bottom*), in the CO group the directionality index *D* evidenced a preferential coupling direction from RR to SAP in the *su* window, and from SAP to RR in the *et* and *lt* windows; the increase from *su* to *et* and from *su* to *lt* was statistically significant. In RNMS patients, the directionality index increased significantly from *su* to *et* and decreased significantly from *et* to *lt*.

The results of causal coupling analysis performed in the information domain over the feedback direction from SAP to RR were supported by the sequence technique in terms of the number of SAP/RR sequences detected in the various conditions. Indeed, as reported in Fig. 5, the total number of baroreflex sequences increased significantly from *su* to *et* in the two groups, whereas during *lt* was maintained in the CO subjects (Fig. 5*A*) and was markedly reduced in the RNMS patients (Fig. 5*B*). Looking at the length of the RR/SAP sequences detected in the different conditions, we found that the increase in the number of sequences from *su* to *et* was associated with a significantly higher number of sequences >3 beats in the CO group (Fig. 5*A*, gray bars) and of 3-beat

sequences in the RNMS group (Fig. 5*B*, gray bars). Moreover, in RNMS patients, the drop of the number of baroreflex sequences upon presyncope was relevant to both 3-beat sequences and longer sequences (Fig. 5*B*, *lt* window).

The results of the interaction delay analysis based on cross-correlation and information theory are shown in Fig. 6. When computed through cross-correlation analysis (Fig. 6*A*), the time delays calculated for the two groups from SAP to RR did not show statistically significant variations across the *su*, *et*, and *lt* windows, whereas a statistically significant difference between *su* and *lt* was observed from RR to SAP only in RNMS patients. As to the delay analysis in the information domain, we

Table 2. *Summary of surrogate data analysis*

	CO Subjects			RNMS Patients		
	su	*et*	*lt*	*su*	*et*	*lt*
$\rho_{SAP \to RR}$	7	10	10	5	10	7
$\rho_{RR \to SAP}$	9	10	8	6	10	8
$C_{SAP \to RR}$	3	7	8	3	8	2
$C_{RR \to SAP}$	8	3	2	5	3	3

Values are the number (out of 10) of CO subjects and RNMS patients for which a statistically significant causal coupling was detected, according to the test based on surrogate data, from SAP to RR and from RR to SAP using cross-correlation analysis ($\rho_{SAP \to RR}$, $\rho_{RR \to SAP}$) or information-domain analysis ($C_{SAP \to RR}$, $C_{RR \to SAP}$) in the *su*, *et*, and *lt* windows.
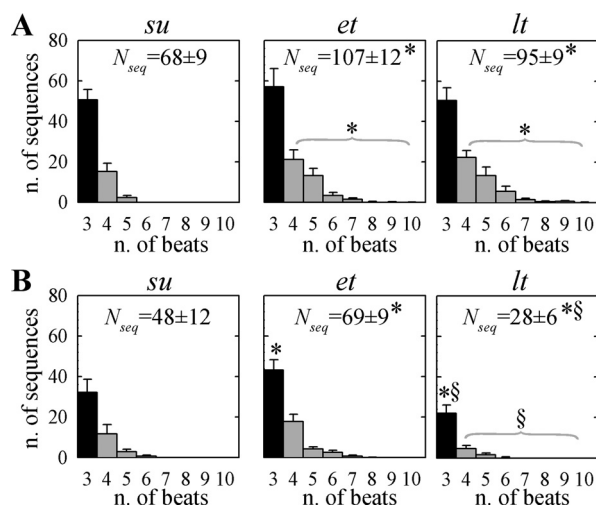

Fig. 5. Distribution of the number of baroreflex sequences of three beats (black) and more than three beats (gray), expressed as means + SE over subjects, computed by sequence analysis for CO subjects (*A*) and RNMS patients (*B*) in *su*, *et*, and *lt* windows of the tilt-test protocol. The total number of baroreflex sequences (N_{seq}, mean ± SE) is reported inside each panel. *Statistically significant difference for *su* vs. *et* or *su* vs. *lt* ($P < 0.05$). §Statistically significant difference for *et* vs. *lt* ($P < 0.05$).
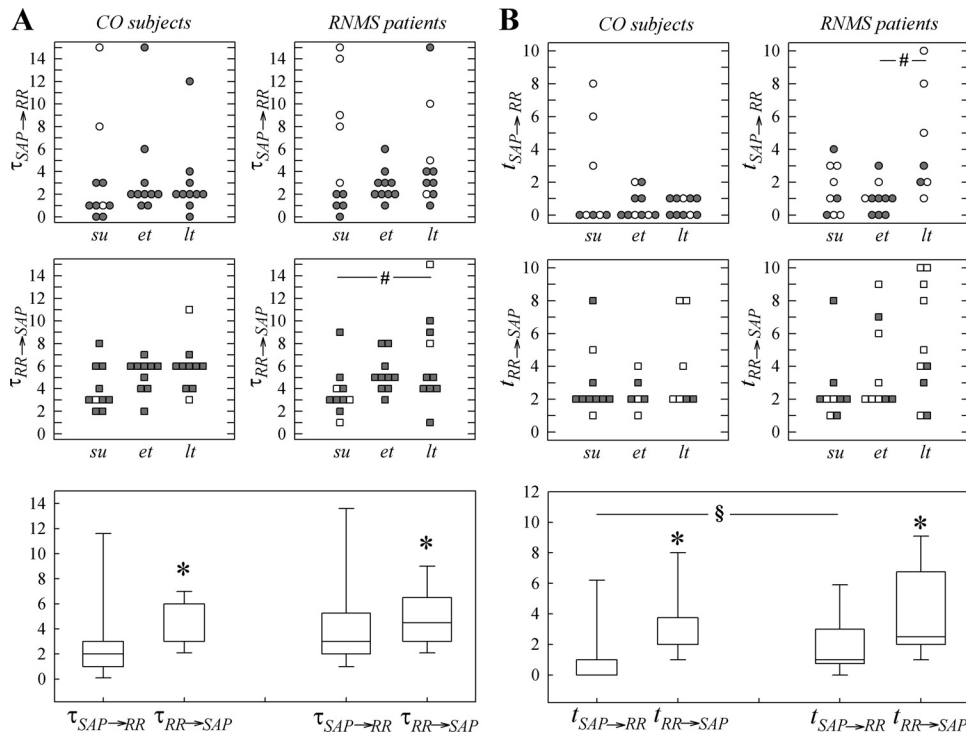
Fig. 6. Results of interaction delay analysis performed by the cross-correlation approach (*A*) and by the information-domain approach (*B*). *Top* and *middle* report the individual values of the time delays from SAP to RR (circles) and from RR to SAP (squares) computed for CO subjects and RNMS patients in *su*, *et*, and *lt* windows of the tilt-test protocol. Filled symbols indicate values for which the causal coupling was detected as statistically significant according to surrogate data analysis. *Bottom* plots report the distribution (box: 25th to 75th percentile; whiskers: 10th to 90th percentiles) of the time delays, pooled across the three windows, estimated in CO subjects (*left*) and RNMS patients (*right*). #Statistically significant difference for *et* vs. *lt* or *su* vs. *lt* ($P < 0.05$). *Statistically significant difference for SAP $\rightarrow$ RR vs. RR $\rightarrow$ SAP ($P < 0.05$). §Statistically significant difference for CO vs. RNMS groups ($P < 0.05$).

observed *1*) the increase of the time delay from SAP to RR in RNMS patients while moving from the *et* to the *lt* window (Fig. 6*B*, *top right*); *2*) after pooling together data from the three windows, a significantly higher delay from SAP to RR in RNMS patients compared with CO subjects (Fig. 6*B*, *bottom*); *3*) a significantly lower interaction delay from SAP to RR than from RR to SAP in both RNMS patients and CO subjects (Fig. 6, *bottom*; this result was observed for both adopted methodological approaches). The same significant variations were observed for the pooled data even when the statistical tests were repeated considering only the time delays computed in the presence of a significant causal coupling (i.e., taking the values denoted by the filled symbols in Fig. 6).

Additionally, we checked the compatibility with the cardiac baroreflex latency of the estimated delays from SAP to RR, considering delays higher than 3 beats as noncompatible with a working baroreflex. The choice of this limit was based on the fact that the time of exhaustion of the effects on the RR interval of single arterial carotid baroreceptor stimuli is <3 s (2). Accordingly, we counted the number of measurements for which the delay was incompatible with a working baroreflex (i.e., with a delay of ≥4 beats), pooling together the two groups and the three analysis windows (60 measures). This number was equal to 17 for the $\tau_{SAP \rightarrow RR}$ measure based on cross-correlation (28%) and equal to 6 for the $t_{SAP \rightarrow RR}$ information-theoretical measure (10%). Furthermore, inside this set of delays incompatible with a working baroreflex, we excluded those found in the presence of uncoupling from SAP to RR. As a consequence, the number of incompatible delays was reduced to nine for the $\tau_{SAP \rightarrow RR}$ measure and to zero for the $t_{SAP \rightarrow RR}$ measure. Therefore, we concluded that the information-domain approach provided delay estimates that did not include values incompatible with the baroreflex latency.

DISCUSSION

The main findings of this study can be summarized in *1*) the demonstration on physiological data of the necessity of dissecting causality between RR and SAP to perform a proper evaluation of the mechanisms involved in cardiovascular regulation, evidenced by the better ability of the proposed information-domain approach to point out modifications when compared with the traditional approach based on CCF; and *2*) the indication of the cardiac baroreflex as a major mechanism involved in the derangement of cardiovascular regulation related to orthostatic syncope, documented by the weakened (i.e., with lower causal coupling) and slowed (i.e., with longer time delays) feedback regulation from SAP to RR observed in RMS patients.

Detection of coupling strength and delay through an information-theoretical approach. In this study, we made use of an information-theoretical approach to the assessment of causality between RR and SAP (11, 12). This approach was specifically devised to deal with the assessment of information transfer in short and noisy physiological time series for which estimating entropy-based measures is normally a daunting task. Specifically, the sequential procedure for non-uniform conditioning overcomes the issues of arbitrariness and redundancy, which may otherwise lead to the detection of spurious causal couplings (11), and the utilization of the CCE estimator compensates for the bias otherwise affecting traditional conditional entropy estimators applied to short time series (31). Once the causal coupling was estimated independently for the feedback and feed-forward directions, the preferential coupling direction was determined as that conveying the largest information transfer through computation of the directionality index. Additionally, utilization of the non-uniform conditioning procedure in which the past terms are not preselected, but are chosen

only if they contribute significantly to the information transfer, allowed us to define new measures of the time delay characterizing the interaction over the investigated causal direction. In this study, the terms causal coupling and delay are used from a physiological point of view to indicate, respectively, the strength of the input-output relation (8, 12) and the apparent postponement of the output with respect to the input (5).

The proposed approach is alternative to traditional approaches characterizing causal interactions between RR and SAP in the time domain through the amplitude and lag of the CCF (41, 47) or in the frequency domain through the modulus and phase of the cross-spectrum (37). Other than the ability to detect nonlinear interactions in addition to the linear interactions captured by these more traditional approaches, the main advantage of our information-theoretical approach is that it is directly linked to the concept of Granger causality (15), according to which a causal effect is detected only when the past history of the time series taken as input effectively helps in describing the present state of the series taken as output. Accordingly, with our approach based on CCE, causality between the two series is not assumed but is tested independently over the two possible directions of interaction so that the resulting coupling and delay measures may reflect both open-loop and closed-loop relations. On the contrary, traditional approaches assume a priori a given causal relation (i.e., an open-loop relation from SAP to RR or vice versa), and this may result in misleading interpretations of coupling strength and delay when the real direction of interaction is opposite to the assumed one or when the two variables interact in a closed loop. Indeed, since the CCF may exhibit periodicities due to coherent oscillations present both in RR and SAP series (e.g., the low-frequency rhythm at 0.1 Hz), the two estimated coupling strengths and the two estimated time delays ($\tau_{SAP \to RR}$ and $\tau_{RR \to SAP}$) are not independent of each other. As a consequence, solely the value compatible with a priori physiological information (e.g., the latency of the cardiac baroreflex) is retained, whereas the other is discarded as unlikely (7, 43). The methodological difficulties of approaches based on cross-correlation or cross-spectrum in detecting time-delayed interactions were pointed out in recent studies (36, 46). In this study, these methodological difficulties were noticed in terms of the less clear physiological interpretation of the results yielded by cross-correlation analysis when compared with the proposed information-domain approach. Indeed, the cross-correlation approach was unable to reveal statistically significant changes in causal coupling and directionality in RNMS patients, whereas the information-domain approach denoted loss of causal coupling from SAP to RR and shift of directionality (Fig. 4). Moreover, as opposed to information-theoretical analysis, cross-correlation did not separate the two groups in terms of estimated delays along the feedback baroreflex pathway (Fig. 6) and detected a considerable number of number of time delays noncompatible with the latency of a working baroreflex.

When applied over the feedback direction, the proposed information-domain approach complements the more traditional approach based on the sequence technique. Indeed, the causal coupling from SAP to RR can be interpreted as a measure of the degree of involvement of the cardiac baroreflex in generating the variability of the heart rate and, as such, is comparable with the number of RR/SAP sequences (either in absolute value or normalized by the number of SAP ramps to

provide the BEI index). Interestingly, in this study, we found very similar variations across conditions for the causal coupling $C_{SAP \to RR}$ and the number of baroreflex sequences N_{seq} in the two groups (Fig. 4B vs. Fig. 5). Moreover, the drop of causal coupling exhibited in the RNMS group upon presyncope was reflected by a consistent decrease of the baroreflex effectiveness as measured by the BEI index. Nevertheless, the information-domain approach might complement the baroreflex sequence technique due to its capability of accounting for nonlinear interactions, thus going beyond linear cross-correlation exploited by baroreflex sequence analysis. In the present study, this possibility was not fully exploited because, probably, nonlinear interactions, if present, are not sufficiently powerful to distinguish the two groups. In addition, the proposed approach provides important information about the feed-forward pathway, hardly distinguishable based on baroreflex sequence analysis.

Feedback and feed-forward cardiovascular regulation in healthy subjects. The results of information-domain analysis of RR-SAP causality performed during different epochs of the adopted tilt-test protocol confirmed the behavior of known physiological mechanisms in healthy subjects. In the resting supine position, we observed an unbalancing of the cardiovascular regulation with a prevalence of the feed-forward direction from RR to SAP over the feedback direction from SAP to RR. This finding was documented by the higher number of subjects showing statistically significant causal coupling over the RR → SAP direction compared with the SAP → RR direction (Table 2) and by the significantly negative values of the directionality index (Fig. 4B). The predominance of feed-forward mechanical mechanisms over the baroreflex feedback at rest confirms previous findings (23–25, 36), which pointed out the necessity of disentangling baroreflex from nonbaroreflex effects in the study of the cardiovascular coupling. When subjects were tilted from the supine to the upright position, the causal coupling increased significantly over the feedback direction and decreased significantly over the feed-forward direction, both in terms of number of coupled subjects and of magnitude of the coupling. The consequent shift of the directionality measure from negative to positive values clearly indicated that the dominant causal direction in the upright position is that going from SAP to RR. This result was also supported by the sequence technique showing an increase in the number of SAP/RR sequences after tilt, and in particular a significantly larger presence of sequences longer than 3 beats documenting a loss of importance of the fast vagal arm in the cardiac baroreflex. Again, this result agrees with previous observations documenting an important involvement of the cardiac baroreflex following the tilt transition, likely related to the unloading of the baroreceptors (7, 29, 36, 43). The unmodified values of causal coupling, directionality, and number of RR/SAP sequences going from *et* to *lt* suggested that, in healthy subjects, the described posture-induced adjustment of the cardiovascular regulation is able to maintain blood pressure within a physiological range even upon prolonged orthostatic position.

Analysis of the interaction delays (Fig. 6) showed that the large majority of RR variations due to SAP are manifested through causal effects, which occur within the same heartbeat (delay equal to zero) or are 1-beat delayed. These values are consistent with previous studies in humans that reported a baroreflex latency of <1 s (2, 3, 30). The delays over the causal

direction from RR to SAP were significantly higher than the delays over the baroreflex pathway. This finding is partially expected due to the convention of the RR and SAP measurements leading to a delay from RR to SAP that cannot be equal to 0. However, the conclusion that mechanical effects whereby alterations in the RR interval affect sequentially end-diastolic volume, stroke volume, cardiac output, and finally arterial pressure take more beats to be effective compared with faster neural effects operating along the cardiac baroreflex needs to be confirmed by including respiration as exogenous input. Indeed, influences of respiration might completely explain this finding, leading to values of the delay from RR to SAP closer to 1 than it appears from this bivariate analysis excluding respiration. We did not find statistically significant variations of the delay from SAP to RR or of the delay from RR to SAP across the three analysis windows, indicating that the underlying mechanisms do not modify their latency in the considered experimental conditions, although the degree of involvement of the two arms of RR-SAP closed loop varies as shown by the reported causal coupling variations.

Feedback and feed-forward cardiovascular regulation in neurally mediated syncope. Utilization of the proposed information-theoretical approach in the group of patients led us to observe specific patterns of modification of the mechanisms of RR-SAP causality in RNMS patients. Similar results in RNMS patients and CO subjects were observed for the two causal coupling measures and for the directionality measure while lying in the supine position and moving to the upright position. By contrast, maintenance of the orthostatic position up to the first symptoms of presyncope was associated with peculiar modifications of these measures (Fig. 4B). Specifically, the drops in the information transfer from SAP to RR (both in terms of coupling magnitude and number of subjects with significant coupling) and in the directionality index suggested a loss of the baroreflex regulation of heart rate in the minutes preceding the decrease of pressure marking the beginning of syncope. The sequence analysis supported this finding, showing a consistent reduction of the number of baroreflex sequences in the lt. Thus the disappearance of causality from SAP to RR preceding the syncope event seems to forewarn the failure of cardiovascular regulation before the appearance of bradycardia and the fall in blood pressure that leads to fainting. This result, which was not clearly evidenced by traditional cross-correlation analysis (Fig. 4A), agrees with previous studies from our group where we noticed a significant decrease of the causal coherence from SAP to RR evaluated in the frequency domain (13) and of the degree of nonlinear predictability of RR given SAP (24) in proximity of presyncope. The findings about the loss of feedback coupling are complemented by the drop in the baroreflex gain documented during postural syncope both in the present study (through the BRS index) and in previous studies (19, 21). Although these two trends are both documenting a dysfunction of the cardiac baroreflex before presyncope, it should be remarked that causal coupling and gain are different measures, describing the cardiac baroreflex, respectively, in terms of the strength of the relation (i.e., the degree of RR-SAP linear and nonlinear correlation) and the magnitude of the linear relation assessing the the RR variation per unit change of SAP. We suggest that, in this case, not only the magnitude of the baroreflex is dampened (depressed sensitivity as measured by BRS), but also the mechanism is

deactivated (absence of causal link from SAP to RR as measured by $C_{SAP \to RR}$ and BEI) in RNMS patients as a consequence of the prolonged postural stress.

Another important result was that RNMS patients showed a significantly longer delay associated with the causal interaction from SAP to RR than CO subjects; moreover, this delay increased significantly in the minutes before presyncope compared with the early phase of head-up tilt (Fig. 5). This higher delay likely reflects a decreased involvement of the fast vagal arm of baroreflex upon late tilt in the RNMS patients, which is also supported by the drops of the RMSSD and HF power of the RR intervals, as well as of the indexes of baroreflex sensitivity and effectiveness provided by the sequence technique (see Table 1). The observation that an increased delay may be related to a reduced parasympathetic activity finds indirect confirmation in the study of Cividjian et al. (5), who showed a reduction in the delay when sympathetic activity is lowered and parasympathetic activity is increased after central sympathetic blockade induced by clonidine. Another potentially dangerous factor is that, during head-up tilt, an overall increase of the delay of the closed loop (i.e., the sum of $\tau_{SAP \to RR}$ and $\tau_{RR \to SAP}$), only partially compensated by the decrease of the baroreflex gain, might lead to the instability of the RR-SAP closed loop, thus being a possible mechanism of syncope (16). The trends of the delay over the feedback pathway were not apparent using traditional cross-correlation analysis. Overall, they support from the point of view of information-domain analysis previous investigations showing an increased lag of occurrence of the maximum correlation in the time domain between short SAP and RR sequences (16) or an increased phase shift in the frequency domain between SAP and RR low-frequency fluctuations (17) in patients with poor orthostatic tolerance.

Limitations and future developments. One important limitation of the present study is that respiration variability data were not available in the collected database. It is well known that respiration affects cardiovascular variability (44, 45) and that causality between RR and SAP may be influenced by the way respiration affects RR and SAP (32, 33). Indeed, when direct respiratory influences on RR are stronger that respiratory influences on SAP, any measured directionality index would be biased toward negative values (causality from RR to SAP). The opposite situation (i.e., tendency to have more positive directionality indexes) would occur when respiratory influences on SAP are stronger than respiratory influences affecting RR independently of SAP. Nevertheless, two remarks should be made about this issue and the proposed information-theoretical approach. First, since the proposed approach is sensitive to the stronger variations in amplitude in the observed signals, it would capture causality between RR and SAP independently of respiratory effects when low-frequency components are dominant in the time series over respiration-related high-frequency components. This should be the case of head-up tilt like in the considered protocol, where sympathetic activation imposes a decrease of respiratory sinus arrhythmia in presence of an increased SAP low-frequency power (7). Second, the original formulation of the method used in this study is fully multivariate, and we have already developed the approach to deal with respiration-related effects on the cardiovascular loop (12). Therefore, future studies should be focused on assessing causality in cardiovascular and cardiorespiratory variability

after including respiration in the acquisition protocol or deriving its variability series from the ECG signal, with application directed to the study of physiological stimuli like in this study and to pharmacological stimuli like very recently suggested (35).

Moreover, we focused on a selected population, that is, a group of otherwise healthy subjects suffering from recurrent syncope. On the other hand, very heterogeneous pictures of orthostatic syncope are commonly observed in a clinical setting, e.g., with profound differences between occasional and recurrent healthy fainters (14, 21). In addition, multiple different mechanisms, not only involving heart rate and arterial pressure relationships, may play a key role in the development of neurally mediated syncope (22). Therefore, our study, by stressing the importance of causality analysis, might open a new perspective toward the description of short-term cardiovascular regulation in patients suffering from syncope.

Perspective and significance. Our results suggest the cardiac baroreflex feedback as a main mechanism involved in the cardiovascular impairment occurring in RNMS patients, thus supporting the baroreflex dysfunction theory of neurally mediated syncope (22). Nevertheless, we stress the importance of applying a method able to investigate effects of directional interactions between heart rate and arterial pressure variability without prior assumptions about which is the preferential direction of interaction. This necessity was illustrated in the present study both from a methodological point of view, showing that the proposed nonlinear and model-free approach to causality assessment performs better than a traditional linear cross-correlation approach, and from a physiological point of view, evidencing that different patterns of causality may be present in different experimental conditions or pathological states. Various alternatives exist to the approach proposed in this study, ranging from linear parametric models studied in time or frequency domains (9, 34) to phase synchronization (26, 38) and nonlinear prediction (24) methods. Since it is framed in information theory and is based on an efficient entropy estimator combined with an objective conditioning procedure (11), our method offers the advantages of being devised to assess short-term variability and of allowing objective estimation of the interaction delay separately for the feedback and feed-forward direction of the investigated closed loop. Since it is readily extensible to the multivariate case, it represents a viable means to explore with a broader perspective the full range of physiological mechanisms involved in postural syncope, e.g., including cardiopulmonary and cerebrovascular effects reflected by respiration and blood-flow velocity signals.

DISCLOSURES

No conflicts of interest, financial or otherwise, are declared by the author(s).

AUTHOR CONTRIBUTIONS

Author contributions: L.F., G.N., and A.P. conception and design of research; L.F. performed experiments; L.F. analyzed data; L.F., G.N., and A.P. interpreted results of experiments; L.F. prepared figures; L.F., G.N., and A.P. drafted manuscript; L.F., G.N., and A.P. edited and revised manuscript; L.F., G.N., and A.P. approved final version of manuscript.

REFERENCES

1. **Barbieri R, Parati G, Saul JP.** Closed-versus open-loop assessment of heart rate baroreflex. *IEEE Eng Med Biol Mag* 20: 33–42, 2001.

2. **Baskerville AL, Eckberg DL, Thompson MA.** Arterial pressure and pulse interval responses to repetitive carotid baroreceptor stimuli in man. *J Physiol* 297: 61–71, 1979.

3. **Borst C, Karemaker JM.** Time delays in the human baroreceptor reflex. *J Auton Nerv Syst* 9: 399–409, 1983.

4. **Brignole M, Alboni P, Benditt D, Bergfeldt L, Blanc JJ, Bloch Thomsen PE, van Dijk JG, Fitzpatrick A, Hohnloser S, Janousek J, Kapoor W, Kenny RA, Kulakowski P, Moya A, Raviele A, Sutton R, Theodorakis G, Wieling W.** Guidelines on management (diagnosis and treatment) of syncope. *Eur Heart J* 22: 1256–1306, 2001.

5. **Cividjian A, Toader E, Wesseling KH, Karemaker JM, McAllen R, Quintin L.** Effect of clonidine on cardiac baroreflex delay in humans and rats. *Am J Physiol Regul Integr Comp Physiol* 300: R949–R957, 2011.

6. **Cohen MA, Taylor JA.** Short-term cardiovascular oscillations in man: measuring and modelling the physiologies. *J Physiol* 542: 669–683, 2002.

7. **Cooke WH, Hoag JB, Crossman AA, Kuusela TA, Tahvanainen KUO, Eckberg DL.** Human response to upright tilt: a window on central autonomic integration. *J Physiol* 517: 617–628, 1999.

8. **Di Rienzo M, Parati G, Castiglioni P, Tordi R, Mancia G, Pedotti A.** Baroreflex effectiveness index: an additional measure of baroreflex control of heart rate in daily life. *Am J Physiol Regul Integr Comp Physiol* 280: R744–R751, 2001.

9. **Faes L, Erla S, Nollo G.** Measuring connectivity in linear multivariate processes: definitions, interpretation, and practical analysis. *Comp Math Methods Med* 2012: 140513, 2012.

10. **Faes L, Nollo G, Chon KH.** Assessment of Granger causality by nonlinear model identification: application to short-term cardiovascular variability. *Ann Biomed Eng* 36: 381–395, 2008.

11. **Faes L, Nollo G, Porta A.** Information-based detection of nonlinear Granger causality in multivariate processes via a nonuniform embedding technique. *Phys Rev E* 83: 051112, 2011.

12. **Faes L, Nollo G, Porta A.** Non-uniform multivariate embedding to assess the information transfer in cardiovascular and cardiorespiratory variability series. *Comput Biol Med* 42: 290–297, 2012.

13. **Faes L, Widesott L, Del Greco M, Antolini R, Nollo G.** Causal cross-spectral analysis of heart rate and blood pressure variability for describing the impairment of the cardiovascular control in neurally mediated syncope. *IEEE Trans Biomed Eng* 53: 65–73, 2006.

14. **Furlan R, Piazza S, Dell'Orto S, Barbic F, Bianchi A, Mainardi L, Cerutti S, Pagani M, Malliani A.** Cardiac autonomic patterns preceding occasional vasovagal reactions in healthy humans. *Circulation* 98: 1756–1761, 1998.

15. **Granger CWJ.** Investigating causal relations by econometric models and cross-spectral methods. *Econometrica* 37: 424–438, 1969.

16. **Gulli G, Claydon VE, Cooper VL, Hainsworth R.** R-R interval-blood pressure interaction in subjects with different tolerances to orthostatic stress. *Exp Physiol* 90: 367–375, 2005.

17. **Gulli G, Cooper VL, Claydon V, Hainsworth R.** Cross-spectral analysis of cardiovascular parameters whilst supine may identify subjects with poor orthostatic tolerance. *Clin Sci (Lond)* 105: 119–126, 2003.

18. **Holm S.** A simple sequential rejective multiple test procedure. *Scand J Statistics* 6: 65–70, 1979.

19. **Iacoviello M, Forleo C, Guida P, Sorrentino S, D'Andria V, Rodio M, D'Alonzo L, Favale S.** Independent role of reduced arterial baroreflex sensitivity during head-up tilt testing in predicting vasovagal syncope recurrence. *Europace* 12: 1149–1155, 2010.

20. **Malpas SC.** Neural influences on cardiovascular variability: possibilities and pitfalls. *Am J Physiol Heart Circ Physiol* 282: H6–H20, 2002.

21. **Mosqueda-Garcia R, Furlan R, Fernandez-Violante R, Desai T, Snell M, Jarai Z, Ananthram V, Robertson RM, Robertson D.** Sympathetic and baroreceptor reflex function in neurally mediated syncope evoked by tilt. *J Clin Invest* 99: 2736–2744, 1997.

22. **Mosqueda-Garcia R, Furlan R, Tank J, Fernandez-Violante R.** The elusive pathophysiology of neurally mediated syncope. *Circulation* 102: 2898–2906, 2000.

23. **Mullen TJ, Appel ML, Mukkamala R, Mathias JM, Cohen RJ.** System identification of closed loop cardiovascular control: effects of posture and autonomic blockade. *Am J Physiol Heart Circ Physiol* 272: H448–H461, 1997.

24. **Nollo G, Faes L, Antolini R, Porta A.** Assessing causality in normal and impaired short-term cardiovascular regulation via nonlinear prediction methods. *Philos Transact A Math Phys Eng Sci* 367: 1423–1440, 2009.

25. **Nollo G, Faes L, Porta A, Antolini R, Ravelli F.** Exploring directionality in spontaneous heart period and systolic pressure variability interactions in

humans. Implications in baroreflex gain evaluation. *Am J Physiol Heart Circ Physiol* 288: H1777–H1785, 2005.

26. **Ocon AJ, Medow MS, Taneja I, Stewart JM.** Respiration drives phase synchronization between blood pressure and RR interval following loss of cardiovagal baroreflex during vasovagal syncope. *Am J Physiol Heart Circ Physiol* 300: H527–H540, 2011.

27. **Papoulis A.** *Probability, Random Variables and Stochastic Processes.* New York: McGraw Hill, 1984.

28. **Parati G, Di Rienzo M, Bertinieri G, Pomidossi G, Casadei R, Grop-pelli A, Pedotti A, Zanchetti A, Mancia G.** Evaluation of the barore-ceptor-heart rate reflex by 24-hour intra-arterial blood pressure monitoring in humans. *Hypertension* 12: 214–222, 1988.

29. **Pedersen M, Madsen P, Klokker M, Olesen HL, Secher NH.** Sympathetic influence on cardiovascular responses to sustained head-up tilt in humans. *Acta Physiol Scand* 155: 435–444, 1995.

30. **Pickering TG, Davies J.** Estimation of the conduction time of the baroreceptor-cardiac reflex in man. *Cardiovasc Res* 7: 213–219, 1973.

31. **Porta A, Baselli G, Lombardi F, Montano N, Malliani A, Cerutti S.** Conditional entropy approach for the evaluation of the coupling strength. *Biol Cybern* 81: 119–129, 1999.

32. **Porta A, Baselli G, Rimoldi O, Malliani A, Pagani M.** Assessing baroreflex gain from spontaneous variability in conscious dogs: role of causality and respiration. *Am J Physiol Heart Circ Physiol* 279: H2558–H2567, 2000.

33. **Porta A, Bassani T, Bari V, Pinna GD, Maestri R, Guzzetti S.** Accounting for respiration is necessary to reliably infer granger causality from cardiovascular variability series. *IEEE Trans Biomed Eng* 59: 832–841, 2012.

34. **Porta A, Bassani T, Bari V, Tobaldini E, Takahashi AC, Catai AM, Montano N.** Model-based assessment of baroreflex and cardiopulmonary couplings during graded head-up tilt. *Comput Biol Med* 42:298–305, 2011.

35. **Porta A, Castiglioni P, Di Rienzo M, Bassani T, Bari V, Faes L, Nollo G, Cividjian A, Quintin L.** Cardiovascular control and time domain Granger causality: insight from selective autonomic blockade. *Philos Transact A Math Phys Eng Sci.* In press.

36. **Porta A, Catai AM, Takahashi AC, Magagnin V, Bassani T, Tobaldini E, van de BP, Montano N.** Causal relationships between heart period and

37. **Saul JP, Berger RD, Albrecht P, Stein SP, Hui Chen M, Cohen RJ.** Transfer function analysis of the circulation: unique insights into cardiovascular regulation. *Am J Physiol Heart Circ Physiol* 261: H1231–H1245, 1991.

38. **Schafer C, Rosenblum MG, Kurths J, Abel HH.** Heartbeat synchronized with ventilation. *Nature* 392: 239–240, 1998.

39. **Schreiber T.** Measuring information transfer. *Phys Rev Lett* 85: 461–464, 2000.

40. **Schreiber T, Schmitz A.** Improved surrogate data for nonlinearity tests. *Phys Rev Lett* 77: 635–638, 1996.

41. **Silvani A, Grimaldi D, Vandi S, Barletta G, Vetrugno R, Provini F, Pierangeli G, Berteotti C, Montagna P, Zoccoli G, Cortelli P.** Sleep-dependent changes in the coupling between heart period and blood pressure in human subjects. *Am J Physiol Regul Integr Comp Physiol* 294: R1686–R1692, 2008.

42. **Task Force of the European Society of Cardiology, and the North American Society of Pacing and Electrophysiology.** Heart rate variability. Standards of measurement, physiological interpretation, and clinical use. *Eur Heart J* 17: 354–381, 1996.

43. **Taylor JA, Eckberg DL.** Fundamental relations between short-term RR interval and arterial pressure oscillations in humans. *Circulation* 93: 1527–1532, 1996.

44. **Toska K, Eriksen M.** Respiration-synchronous fluctuations in stroke volume, heart rate and arterial pressure in humans. *J Physiol* 472: 501–512, 1993.

45. **Triedman JK, Saul JP.** Blood pressure modulation by central venous pressure and respiration. Buffering effects of the heart rate reflexes. *Circulation* 89: 169–179, 1994.

46. **Wessel N, Suhrbier A, Riedl M, Marwan N, Malberg H, Bretthauer G, Penzel T, Kurths J.** Detection of time-delayed interactions in biosignals using symbolic coupling traces. *Eur Phys Lett* 87: 2009.

47. **Westerhof BE, Gisolf J, Karemaker JM, Wesseling KH, Secher NH, van Lieshout JJ.** Time course analysis of baroreflex sensitivity during postural stress. *Am J Physiol Heart Circ Physiol* 291: H2864–H2874, 2006.

systolic arterial pressure during graded head-up tilt. *Am J Physiol Regul Integr Comp Physiol* 300: R378–R386, 2011.